

Toward an Understanding of the Turbidity Measurement of Heterocoagulation Rate Constants of Dispersions Containing Particles of Different Sizes

Jie Liu, Shenghua Xu, and Zhiwei Sun*

Institute of Mechanics, Chinese Academy of Sciences, Beijing 100080, PR China

Received May 16, 2007. In Final Form: August 27, 2007

Our previous studies have shown that the determination of coagulation rate constants by turbidity measurement becomes impossible for a certain operating wavelength (that is, its blind point) because at this wavelength the change in the turbidity of a dispersion completely loses its response to the coagulation process. Therefore, performing the turbidity measurement in the wavelength range near the blind point should be avoided. In this article, we demonstrate that the turbidity measurement of the rate constant for coagulation of a binary dispersion containing particles of two different sizes (heterocoagulation) presents special difficulties because the blind point shifts with not only particle size but also with the component fraction. Some important aspects of the turbidity measurement for the heterocoagulation rate constant are discussed and experimentally tested. It is emphasized that the T-matrix method can be used to correctly evaluate extinction cross sections of doublets formed during the heterocoagulation process, which is the key data determining the rate constant from the turbidity measurement, and choosing the appropriate operating wavelength and component fraction are important to achieving a more accurate rate constant. Finally, a simple scheme in experimentally determining the sensitivity of the turbidity changes with coagulation over a wavelength range is proposed.

I. Introduction

The coagulation of polydisperse dispersions (heterocoagulation) actually occurs for a broad range of applications, although homocoagulation has been studied more thoroughly. This situation is associated with the fact that heterocoagulation exhibits more complicated behavior and is therefore more difficult to study through modeling. In this regard, as a relatively simple example, the heterocoagulation of two differently sized colloidal particles has received significant attention.^{1–14} The heterocoagulation rate constant is an important parameter for characterizing the coagulation kinetics of colloidal systems. To determine its absolute rate constant, the turbidity measurement is widely adopted because of its simplicity and ease of implementation.^{1–10} This study will focus on the turbidity measurement for the heterocoagulation rate constant of dispersions composed of two differently sized colloidal particles.

Some of the major points presented in previous studies^{15–16} on the turbidity measurement of homocoagulation that are relevant

to the present work can be highlighted by the following points: (a) to achieve a more accurate absolute rate constant, the use of larger particles is preferable; (b) the degree of response of the turbidity change to the coagulation varies significantly with particle size and operating wavelength; at a certain wavelength, the change in turbidity completely loses its sensitivity to the coagulation process (the so-called blind point), which makes the measurement impossible; and (c) the T-matrix method provides a robust solution to the evaluation of the extinction cross section of the doublet, which is the key factor for achieving the coagulation rate constant from the turbidity measurement. These points are also valid for the heterocoagulation measurement in principle.

In this article, we first present a theoretical basis for the connection of the rate constant with the rate of turbidity change in the heterocoagulation process. We also analyze why the significant difference in the responses of the turbidity change to the coagulation for differently sized colloidal particles complicates the turbidity measurement. In particular, for some wavelength zones (blind zones) turbidity does not respond or has a very low response to coagulation, resulting in the impossibility of measuring the rate constant. Furthermore, this blind zone shifts with particle size and component fraction. Then experiments on the turbidity measurement for both homocoagulation and heterocoagulation rate constants with the extinction cross sections of doublets evaluated by the T-matrix method are described, and the relevant results are discussed. Meanwhile, some approaches to improving the accuracy of the turbidity measurement are proposed. Finally, we propose a simple scheme to yield a rough-and-ready curve of the rate of turbidity change versus wavelength that is useful in selecting an appropriate wavelength for the turbidity measurement.

II. Theoretical Basis and Analysis

1. Theoretical Basis. For homocoagulation, in a very early stage of the coagulation process of a monodisperse colloidal system, only collisions of single particles to form doublets need to be considered. Therefore, the change in particle number concentrations can be approximately expressed as

* To whom correspondence should be addressed. E-mail: sunzw@imech.ac.cn.

- (1) Maroto, J. A.; de las Nieves, F. J. *J. Colloid Polym. Sci.* **1999**, *277*, 881.
- (2) Maroto, J. A.; de las Nieves, F. J. *Colloids Surf., A* **1995**, *96*, 121.
- (3) Puertas, A. M.; Maroto, J. A.; Fernandez-Barbero, A.; de Las Nieves, F. J. *Colloids Surf., A* **1999**, *151*, 473.
- (4) Furusawa, K.; Anzai, C. *Colloids Surf.* **1992**, *63*, 103.
- (5) Matijevic, E.; Kitazawa, Y. *Colloid Polym. Sci.* **1983**, *261*, 527.
- (6) Uricanu, V.; Eastman, J. R.; Vincent, B. J. *Colloid Interface Sci.* **2001**, *233*, 1.
- (7) Galletto, P.; Lin, W.; Borkovec, M. *Phys. Chem. Chem. Phys.* **2005**, *7*, 1464.
- (8) Hidalgo-Alvarez, R.; Martin, A.; Fernandez, A.; Bastos, D.; Martinez, F.; de las Nieves, F. J. *Adv. Colloid Interface Sci.* **1996**, *67*, 1.
- (9) Hogg, R.; Healy, T. W.; Fuerstenau, D. W. *J. Chem. Soc., Faraday Trans.* **1996**, *62*, 1638.
- (10) Barouch, E.; Matijevic, E.; Ring, T. A.; Finlan, J. M. *J. Colloid Interface Sci.* **1978**, *67*, 1.
- (11) Islam, A. M.; Chowdhry, B. Z.; Snowden, M. J. *Adv. Colloid Interface Sci.* **1995**, *62*, 109.
- (12) Wang, Q. *J. Colloid Interface Sci.* **1995**, *150*, 418.
- (13) Maroto, J. A.; de las Nieves, F. J. *Colloids Surf., A* **1998**, *132*, 153.
- (14) Yu, W. L.; Matijevic, E.; Borkovec, M. *Langmuir* **2002**, *18*, 7853.
- (15) Sun, Z. W.; Liu, J.; Xu, S. H. *Langmuir* **2006**, *22*, 4946.
- (16) Xu, S. H.; Liu, J.; Sun, Z. W. *J. Colloid Interface Sci.* **2006**, *304*, 107.

$$\left(\frac{dN_S}{dt}\right)_{t=0} = -K_D N_0^2 \quad (1)$$

$$\left(\frac{dN_D}{dt}\right)_{t=0} = \frac{K_D N_0^2}{2} \quad (2)$$

where N_S and N_D are the number concentrations of single particles and doublets, respectively; t is time; K_D is the coagulation rate constant, and $N_0 = (N_S)_{t=0}$.

The turbidity can be expressed as $\tau = N_S C_S + N_D C_D$, where C_S and C_D are the extinction cross sections for single particles and doublets, respectively, and τ is the turbidity. The rate of turbidity change due to the aggregation of single particles is written as

$$\frac{d\tau}{dt} = C_S \frac{dN_S}{dt} + C_D \frac{dN_D}{dt} = \left(\frac{C_D}{2} - C_S\right) K_D N_0^2 \quad (3)$$

From eq 3, the coagulation rate constant can be connected with the rate of turbidity change in the turbidity measurement by the following equation^{17–19}

$$K_D = \frac{[d(\tau/\tau_0)/dt]_0}{[(C_D/2C_S) - 1]N_0} \quad (4)$$

where $\tau_0 = N_0 C_S$ is the turbidity at the coagulation starting time of $t = 0$. Assuming that the denominator in eq 4 can be taken to be a constant, the coagulation rate will be proportional to the quantity $R = [d(\tau/\tau_0)/dt]_0$, the relative rate of turbidity change. Thus $|R|$ is usually used to represent the relative coagulation rate. The dimensionless parameter $F = [(C_D/2C_S) - 1]$ is referred to as the optical factor. R can be obtained from the turbidity measurement, but the optical factor containing the extinction cross sections for single particles and doublets has to be calculated by means of light-scattering theory.

With a similar deduction as in eqs 1–3, the relationship of the rate of turbidity change with the rate of the heterocoagulation coagulation process of species 1 and 2 is given as^{1–3}

$$\left(\frac{d\tau}{dt}\right)_{0,\text{HET}} = \left(\frac{1}{2}C_{D1} - C_{S1}\right)K_{D1}N_1^2 + \left(\frac{1}{2}C_{D2} - C_{S2}\right)K_{D2}N_2^2 + 2K_{D12}N_1N_2\left(\frac{1}{2}C_{D12} - \frac{1}{2}C_{S1} - \frac{1}{2}C_{S2}\right) \quad (5)$$

where N_1 and N_2 are the initial numbers of singlet species 1 and 2, respectively. C_{S1} , C_{S2} , C_{D1} , and C_{D2} are the extinction cross sections of a singlet and a doublet of species 1 and 2, and C_{D12} is the extinction section of a 1:2 doublet. K_{D1} and K_{D2} are the homocoagulation rate constants for particles 1 and 2, respectively, and K_{D12} is the rate constant for doublets formed by two unlike particles. Apparently, eq 5, just like eqs 1–3, holds only for $t \rightarrow 0$, namely, only at the very beginning of the coagulation process.

2. Calculation of Extinction Cross Sections. For spheres, the extinction cross section can be calculated exactly from Mie theory without a size limit. The key problem in determining a reliable value of the absolute coagulation rate constant by the turbidity experiment is to calculate the extinction cross sections for three kinds of doublets, namely, C_{D1} , C_{D2} , and C_{D12} . It has been shown^{15–18} that all previous theories, including Rayleigh–

Gans–Debye (RGD) theory, Mie theory with the coalescing assumption, RGD with the coalescing assumption, and corrected RGD theory,^{17–18} are valid only for rather small colloidal particles. Although this size limitation can be relaxed to some extent when the difference in the refractive indices for colloidal particles and the surrounding medium is small, these theories are basically not suitable for large particles. It has been estimated⁷ that for the measurement of heterocoagulation rate constants with static light scattering or dynamic light scattering, RGD theory is typically applicable to particles having a diameter from 0.1 to 0.2 μm . Some of the previous theories, however, have been applied to the turbidity measurement of heterocoagulation containing large particles.^{20–22} For instance, You-Im Chang et al. studied the heterocoagulation behavior of a binary mixture composed of different combinations of 1.16, 3.04, and even 6.2 μm polystyrene particles. However, the calculation of the extinction cross section in their study is based on the RGD theory that is incapable of dealing with large particles.

Heterocoagulation experiments with large particles are an important aspect of colloidal coagulation fields. For example, studies of sedimentation phenomena showed that the presence of large particles in a dispersion mixture will influence the whole heterocoagulation process remarkably.^{20–23}

To avoid the difficulties involved in the calculation of extinction cross sections of doublets, a technique⁷ using simultaneous static and dynamic light scattering has been developed to determine heterocoagulation rate constants. Currently, however, this technique can treat only the heterocoagulation process between unlike particles, excluding the simultaneous occurrence of homocoagulation.

The T-matrix method has shed new light on dealing with the calculation of extinction cross sections of a doublet formed by large particles²⁴ because it has great capability in accurately computing electromagnetic scattering by single and compounded particles without a size or shape limit. In this study, the T-matrix method was used to calculate all extinction cross sections that are needed in measuring the heterocoagulation rate constant by the turbidity measurement.

In the T-matrix method, both incident and scattered electric fields are expanded in a series of vector spherical wave functions. The scattered field coefficients are related to the incident field coefficients by means of the so-called transition matrix \mathbf{T} (or T matrix), and the extinction cross section can be calculated from \mathbf{T} of the scattering object.²⁴

For a spherical particle, the T matrix is diagonal, and its elements are directly related to Mie coefficients a_n and b_n from Mie scattering.²⁴ And the T matrix for an aggregate formed by two particles (regardless of whether they are the same size) can be deduced from the T matrices of each particle, which has been discussed in detail in refs 15 and 16. Therefore, all of the extinction cross sections in eq 5 can be accurately calculated by the T matrix method.

3. Analysis. According to eq 5, we can see that the rate of turbidity change is determined by three terms and that each of them has a form similar to eq 3. The first two terms correspond to the contributions of two like-sized spherical particles forming a doublet, and the third term represents the contribution due to doublet formation between two unlike-sized spheres. As discussed

(17) Lichtenbelt, J. W. Th.; Ras, H. J. M. C.; Wiersema, P. H. *J. Colloid Interface Sci.* **1974**, *46*, 562.

(18) Lichtenbelt, J. W. Th.; Pathmanmanoharan, C. *J. Colloid Interface Sci.* **1974**, *49*, 281.

(19) Elimelech, M.; Gregory, J.; Jia, X. et al. *Particle Deposition and Aggregation*; Butterworth-Heinemann: Oxford, U.K., 1995.

(20) Chang, Y. I.; Wang, M. C. *Colloids Surf., A* **2004**, *251*, 75.

(21) Melik, D. H.; Fogler, H. S. *J. Colloid Interface Sci.* **1984**, *101*, 72.

(22) Maroto, J. A.; de las Nieves, F. J. *Colloids Surf., A* **1998**, *145*, 271.

(23) Sun, Z. W.; Liu, J. *Chin. Phys. Lett.* **2005**, *22*, 2119.

(24) Mishchenko, M. I.; Travis, L. D.; Lacis, A. A. *Scattering, Absorption, and Emission of Light by Small Particles*; Cambridge University Press: Cambridge, U.K., 2002.

in ref 15 for the homocoagulation case, each term may vary dramatically with the incident light wavelength λ : not only is its magnitude very different at different λ but its sign also may change from negative through zero to positive. When two primary particles are combined to form a doublet during coagulation, there will be a corresponding change in their extinction sections. If the extinction section of two singlets is less than that of one doublet, then we will have $(d\tau/dt) > 0$; otherwise, $(d\tau/dt) < 0$. And the case of $(d\tau/dt) = 0$ corresponds to the extinction section of two singlets that is equal to that of one doublet. If the measurement is performed at the λ with $(d\tau/dt) \approx 0$, then $(d\tau/dt)$ will have no response to the actual coagulation process. In this case, the change in turbidity during coagulation completely loses its sensitivity to the change in particle number N of the dispersions. Within this zone (the zero-sensitivity zone or the blind zone), the magnitude of the slope of the $\tau - t$ curve at $t = 0$ is too small to distinguish. (The signal is covered by noise.) Apparently, for heterocoagulation, the situation becomes much more complicated because the summation of the three terms in eq 5 still can be zero (they may take different signs) although each of them is nonzero. In this case, the value of $(d\tau/dt)$ will depend not only on the values of all extinction sections of primary particles and doublets but also on the fraction of species 1 and 2. Furthermore, extinction cross sections are related to particle size and the operating wavelength. Our target is to achieve the heterocoagulation rate constant for doublets formed by unlike-sized particles, K_{D12} , through the turbidity measurement and theoretical values of all relevant extinction cross sections. From eq 5, K_{D12} can be explicitly expressed by the following equation

$$K_{D12} = \frac{A - B - C}{DN_1N_2} \quad (6)$$

where

$$A = \left(\frac{d\tau}{dt}\right)_{0,\text{HET}}$$

$$B = \left(\frac{1}{2}C_{D1} - C_{S1}\right)K_{D1}N_1^2$$

$$C = \left(\frac{1}{2}C_{D2} - C_{S2}\right)K_{D2}N_2^2$$

and

$$D = (C_{D12} - C_{S1} - C_{S2})$$

The numerator $(A - B - C)$ on the right-hand side (RHS) of eq 6 corresponds to the rate of turbidity change caused only by doublet formation between two unlike particles. The three terms, A , B , and C , can be experimentally determined by turbidity measurements, but D has to be estimated theoretically.

There are two approaches to obtain B and C . The first one is based on the fact that B and C represent the rates of turbidity change of monodisperse dispersion species 1 and 2, respectively (eq 3). Therefore, each of them can be directly measured by separate experiments. This method does not require either the values of the absolute rate constants (K_{D1} , K_{D2}) or calculations of the relevant extinction cross sections. The disadvantage of this method is that the turbidity measurements for $(d\tau/dt)_{0,1}$ and $(d\tau/dt)_{0,2}$ have to be performed with exactly the same particle number concentrations at exactly the same operating wavelength as those for measuring $(d\tau/dt)_{0,\text{HET}}$ (the rate of turbidity change for the mixture of species 1 and 2). Apparently, it is difficult to obtain $(d\tau/dt)_{0,\text{HET}}$, $(d\tau/dt)_{0,1}$, and $(d\tau/dt)_{0,2}$ with sufficient accuracy

by performing the measurements at the same operating wavelength because each of them may have a very different measuring sensitivity at the same wavelength.

In opposition to the first method, the second one has to resort to attaining values of the absolute rate constants, K_{D1} and K_{D2} , as well as all relevant extinction cross sections. Because K_{D1} and K_{D2} are independent of the operating wavelength for the measurement, as long as all extinction cross sections required in eq 6 can be correctly estimated, we can choose proper wavelengths for the rate constant measurements (K_{D1} and K_{D2}) that are individually suitable for species 1 and 2.

For the A term, the situation becomes much more complicated. First, the wavelength blind point for the mixture of species 1 and 2 will shift not only with the particle sizes but also with the fraction of two species. Let the component fraction $X = N_2/(N_1 + N_2)$ (N_1 and N_2 are the number concentrations of two types of particles, respectively). In the initial stage of the heterocoagulation, doublets in dispersion solution can be formed by two like particles or two unlike (dissimilar) particles. Apparently, more doublets composed of two unlike particles in solution would enhance the accurate determination of K_{D12} . Mathematically, the maximum possible number of such doublets should come about when $X = 0.5$ (namely, $N_1 = N_2$). However, $X = 0.5$ may not be a good choice for the component fraction because the intensity of light scattered on dispersion particles strongly depends on the particle size. According to Rayleigh's theory, that holds for particles much smaller than the wavelength of light because the scattering of light by particles is proportional to particle size to the sixth power. Therefore, when $N_1 = N_2$, the turbidity contribution from larger particles may greatly mask that from smaller ones, resulting in large experimental errors.

Interestingly, if the wavelength of the blind point can be somehow determined, to achieve K_{D12} one needs to know only B and C in eq 6 because $A = 0$.

III. Experimental Section

Three types of negatively charged polystyrene (PS) spheres of radii equal to $a = 115$, 266, and 500 nm were used in both the homo- and heterocoagulation measurements in this work, and they are denoted as PS115, PS266, and PS500, respectively, in the following discussions. The initial particle number concentration of stock solution was determined according to particle size and the dry weight of the dispersions of a certain amount of sample solution. The estimated error associated with the number concentration was about 5%. Two series of binary mixtures (denoted as mix 1 and mix 2) were used in the heterocoagulation experiments: mix 1 was composed of compounds with PS115 and PS266, whereas mix 2 was composed of PS266 and PS500.

Transmission percentages ($T\%$) of samples versus time during the homo- and heterocoagulation processes at different wavelengths were measured by a UV-vis dual-beam spectrophotometer (Purkinje TU-1901, Beijing) connected to a computer for all data collection. Then, the transmission percentages were transformed into turbidity by the equation

$$\tau = -\left(\frac{1}{L}\right)(\ln T\%) \quad (7)$$

where L is the light-path length. The slope of the τ/τ_0 versus time curve (the relative coagulation rate) was calculated by the procedure of linear regression in the early stage of the coagulation. All results presented below are the values averaged over five independent experiments.

Before the measurements began, the containers for the electrolyte and latex solution as well as the sample cells were cleaned with a chromium sulfuric acid solution in order to eliminate organic materials. The use of any detergent-based cell cleaning solution was

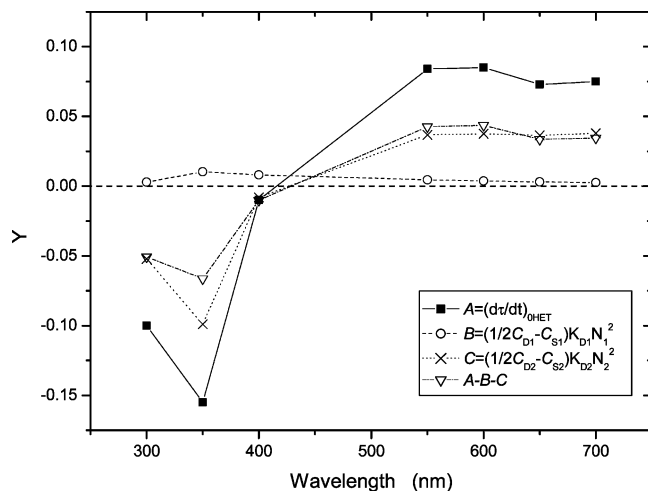


Figure 1. Change in terms A , B , C , and $(A - B - C)$ in eq 6 for sample mix 1 with component fraction $X = 0.5$ vs the operating wavelength.

Table 1. Number Concentrations and Volume Fractions of Particles for Different Dispersion Solutions Used in This Study

		1:1		5:1	
		N (10^{14} p/m 3)	Φ (10^{-5})	N (10^{14} p/m 3)	Φ (10^{-5})
mix 1	PS115	6.25	0.397	10.4	0.66
	PS266	6.25	4.92	2.08	1.64
	total	12.5	5.32	12.5	2.30
mix 2	PS266	2.0	1.57	3.33	2.62
	PS500	2.0	10.0	0.67	3.48
	total	4.0	11.6	4.0	6.1

avoided because the coagulation rate constant is sensitive to the presence of trace amounts of surfactants. The water was obtained from an ion-exchange apparatus, and the conductivity was lower than $0.5 \mu\text{S}/\text{cm}$.

The experiments were performed at a temperature of $T = 25^\circ\text{C}$, and for each sample, the fast coagulation was initiated by mixing 1 mL of 1 M NaCl solution with 1 mL of latex solution in the sample cell (the length that light passed through the dispersion was 10 mm) for all of the experiments. The critical coagulation concentrations for particles PS115, PS266, and PS500 are 0.3, 0.34, and 0.32 M, respectively; therefore, the electrolyte concentration used here is sufficiently higher than the required critical coagulation concentration. The final total number particle concentrations in the cell after being mixed with electrolyte solution for mix 1 and mix 2 were 1.25×10^{15} and $4 \times 10^{14}/\text{m}^3$, respectively. More detailed information about the number concentration N and volume fraction Φ of three kinds of particles in different mixtures is shown in Table 1.

IV. Results and Discussion

1. A , B , C ($A - B - C$) in Equation 6 versus Wavelength and Their Blind Points. Figure 1 shows the change of the terms A , B , C and $(A - B - C)$ in eq 6 for sample mix 1 with the component fraction $X = 0.5$ versus the operating wavelength. To achieve the values of B and C according to eq 3, K_{D1} and K_{D2} were determined through separate turbidity measurements performed at appropriate operating wavelengths by the procedure described in ref 15. We can see that with the wavelength increase from 300 to 700 nm all A , C , and $(A - B - C)$ experience a negative-to-positive sign change. For each term, its blind point corresponds to its value of zero. Because the blind point for term B is at a wavelength of less than 300 nm, we cannot see its sign change in Figure 1.

Figure 2 presents similar behavior for the sample of mix 2 (also with the component fraction $X = 0.5$). Now we can see that

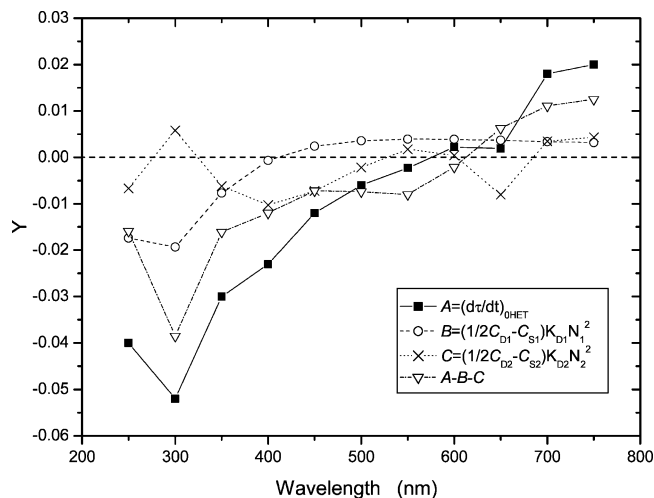


Figure 2. Change in terms A , B , C , and $(A - B - C)$ in eq 6 for sample mix 2 with component fraction $X = 0.5$ vs the operating wavelength.

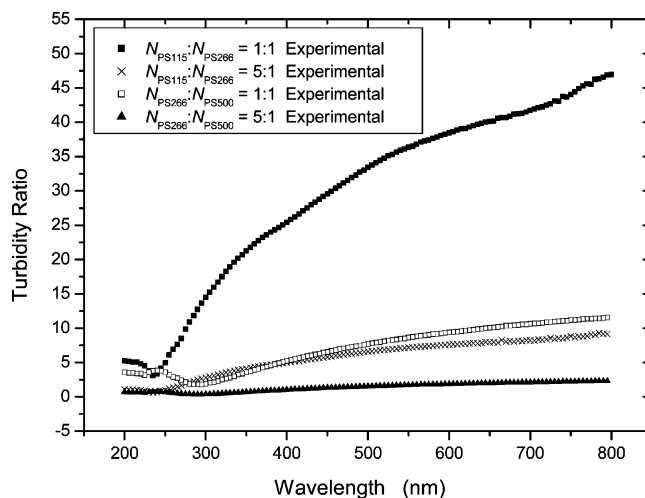


Figure 3. Turbidity vs wavelength of the incident light beam for dispersions composed of PS115, PS266, and PS500, respectively. In all three cases, the same number concentration of particles is used ($2 \times 10^8/\text{cm}^3$).

all terms A , B , C , and $(A - B - C)$ have their blind points in the range of wavelength between 300 and 700 nm.

2. Turbidity Contribution of Differently Sized Particles.

As discussed above, the turbidity of a dispersion drops violently with a decrease in the size of particles in the dispersion.

Figure 3 contains the plot of the wavelength-dependent turbidity ratios of a dispersion of PS266 to that of PS115 ($\tau_{\text{PS266}}/\tau_{\text{PS115}}$) for their number concentration ratio $N_{\text{PS266}}/N_{\text{PS115}} = 1:1$ and 1:5, respectively, and also the plot for the ratios of PS500 to PS266 ($\tau_{\text{PS500}}/\tau_{\text{PS266}}$) for $N_{\text{PS500}}/N_{\text{PS266}} = 1:1$ and 1:5, respectively.

We can see that the turbidity of a dispersion composed of larger particles has a much greater value than that of a dispersion composed of smaller particles. This implies that if the same number concentrations of larger and smaller particles (namely, $X = 0.5$) in the turbidity measurement of heterocoagulation are used the contribution of larger particles would greatly mask that of smaller ones, resulting in large experimental errors. Figure 3 also shows that a useful remedy to this situation is to increase the content of smaller particles.

Figure 3 does not seem to show that the turbidity of the dispersion is proportional to particle size to the sixth power, as discussed above; this is because the sizes of particles here are

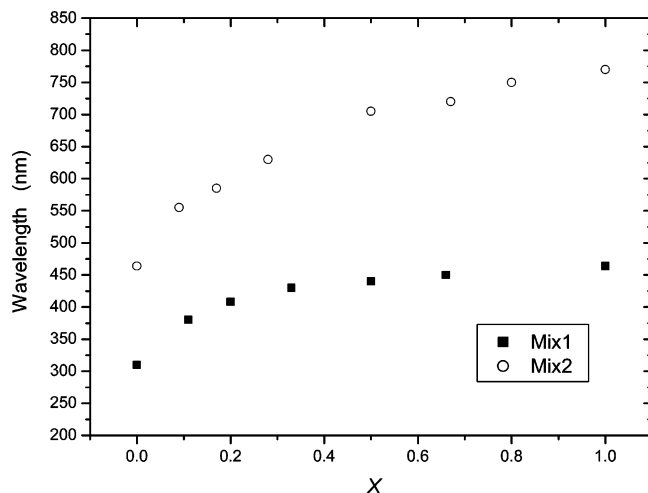


Figure 4. Wavelength-dependent turbidity ratios of PS266 to PS115 ($\tau_{\text{PS266}}/\tau_{\text{PS115}}$) with the number concentration ratio $N_{\text{PS115}}/N_{\text{PS266}} = 1:1$ and $5:1$ and wavelength-dependent turbidity ratios of PS500 to PS266 ($\tau_{\text{PS500}}/\tau_{\text{PS266}}$) for number concentration ratio $N_{\text{PS266}}/N_{\text{PS500}} = 1:1$ and $5:1$.

too large (compared to the wavelength) to meet the condition of Rayleigh theory. We still can see, however, the tendency that the turbidity ratio of larger particles to smaller ones increases with the increase in wavelength because a larger wavelength makes the particle sizes move toward the Rayleigh condition.

Figure 3 also shows that the disparity in turbidity contributions from large and small particles becomes greater when the studied particle sizes are small. The turbidity ratios of the dispersion of PS266 to that of PS115 ($\tau_{\text{PS266}}/\tau_{\text{PS115}}$) is greater than 40 at a wavelength of $\lambda = 700$ nm. But this ratio for PS500 to PS266 ($\tau_{\text{PS500}}/\tau_{\text{PS266}}$) is only about 10 at $\lambda = 700$ nm.

Actually, Figure 3 also demonstrates the advantage of using larger particles in turbidity measurement.¹⁵

3. Wavelength of the Blind Point versus Component Fraction for Heterocoagulation. It is important to know the position (wavelength) of the blind point in the turbidity measurement of the rate constant.¹⁵ For homocoagulation, the position of the blind point is definite, but for the heterocoagulation, the blind point shifts with the component fraction. For monodisperse dispersions of PS115, PS266, and PS500, their blind points are 310, 464, and 770 nm, respectively. Figure 4 shows how the position of the blind point shifts with component fraction for mix 1 and mix 2. For mix 1, when the component fraction of smaller particles PS266 increases from $X = 0$ to 1, its blind point shifts from 464 nm (the value for the blind point of PS115) to 310 nm (the value for the blind point of PS266). For mix 2, when the component fraction of PS500 increases from $X = 0$ to 1, this shift is from 770 to 464 nm. We can see that for both cases, with an increase in the portion of smaller particles, the blind point first moves toward a short wavelength (approaching the blind point of smaller particles) at a fast pace and then slows down. This fact implies that the larger particles play a leading role. Apparently, this trend is displayed more significantly for mix 1 because its particles are smaller and fit the Rayleigh scattering better.

4. Extinction Cross Sections. Figure 5 presents the values of D in eq 6 calculated from the T-matrix method at different wavelengths. Because the heterocoagulation rate constant is independent of the measuring wavelength, the numerator ($A - B - C$) and the denominator on D on the RHS of eq 6 have to be complementary to each other to ensure that the rate constant is constant over the whole operating wavelength range. That is,

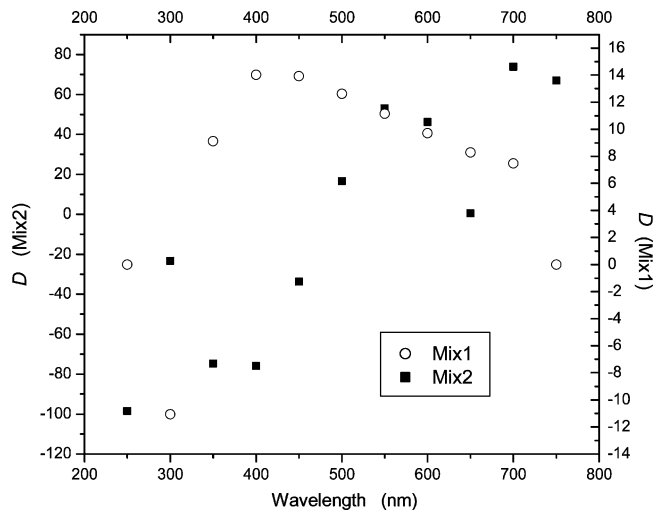


Figure 5. Values of D in eq 6 calculated from the T-matrix method at different wavelengths. Note that doubled scales were used: the left ordinate axis is for mix 2, and the right axis is for mix 1.

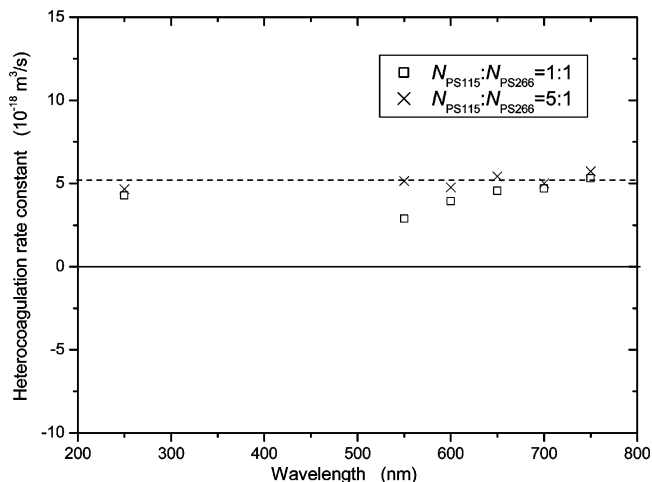


Figure 6. Absolute heterocoagulation rate constants of mix 1 obtained from the turbidity measurement at different operating wavelengths.

$(A - B - C)/D$ should be unchanged, within the error bar, with the wavelength. Comparing the curves of D in eq 7 with those of $(A - B - C)$, we can see that they are basically complementary (except for some lack of experimental data near the blind points (values for the blind point).

In addition, the correctness of the relevant cross sections in eq 6 evaluated by the T-matrix method can be essentially verified by the final results of absolute heterocoagulation rate constants reported in the next part.

5. Absolute Heterocoagulation Rate Constants. As discussed in ref 15 for the same sample of dispersions, the coagulation rate constants evaluated by eq 6 in turbidity measurement performed at different wavelengths have to be unaltered and unique. We can still use this criterion to evaluate our experimental results obtained by different implementation methods.

The absolute heterocoagulation rate constants of the mix 1 and mix 2 mixture obtained from the turbidity measurement at different operating wavelengths are presented in Figures 6 and 7, respectively. For both cases, two kinds of component fractions were used: $N_1/N_2 = 1:1$ and $N_1/N_2 = 5:1$. Figure 6 shows the data points for mix 1. We can see that when $\lambda > 550$ nm the data of the rate constants with $N_{\text{PS115}}/N_{\text{PS266}} = 5:1$ measured at different wavelengths are consistent and also compatible with the

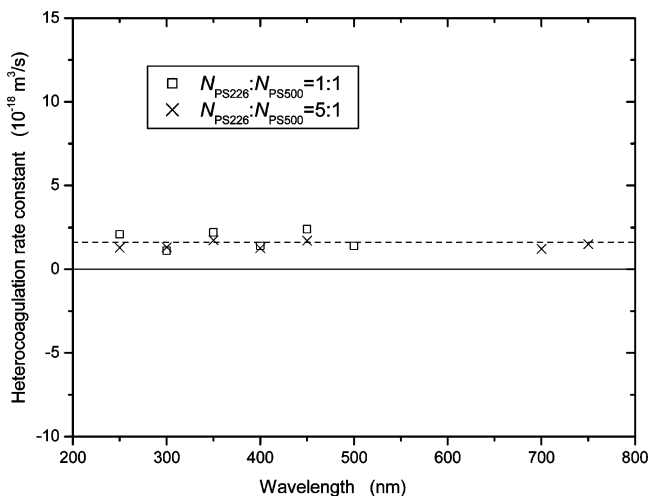


Figure 7. Absolute heterocoagulation rate constants of mix 2 obtained from the turbidity measurement at different operating wavelengths.

Table 2. Homo- and Heterocoagulation Rate Constants of Different Dispersions

sample	PS115	PS266	PS500	mix 1	mix 2
$K_D (10^{-18} \text{ m}^3/\text{s})$	6.2(± 0.6)	3.0(± 0.4)	3.4(± 0.4)	5.2(± 0.6)	2.0(± 0.2)

heterocoagulation rate constants reported by other researchers.^{1–10} Figure 6 also shows that a larger deviation of data points occurs in the $N_{\text{PS115}}/N_{\text{PS266}} = 1:1$ case. The blind point is around 440 nm for $N_{\text{PS115}}/N_{\text{PS266}} = 1:1$ and around 400 nm for $N_{\text{PS115}}/N_{\text{PS266}} = 5:1$. Therefore, there is an uncertain zone for turbidity measurement from 300 nm to 500 nm. We can see the data returned again to the average value at the wavelength around 250 nm. Some data points in a rather wide range around blind points are not given in Figures 6 and 7 because they could not be determined with an acceptable accuracy there (the values of $d\tau/dt$ near blind points are too small to measure).

Figure 7 presents the data points for mix 2 having the blind point around 705 nm for $N_{\text{PS266}}/N_{\text{PS500}} = 1:1$ and 585 nm for $N_{\text{PS266}}/N_{\text{PS500}} = 5:1$. We can see that the data are consistent with the range from 250 to 500 nm for $N_{\text{PS266}}/N_{\text{PS500}} = 1:1$ and from 250 to 450 nm plus that from 700 to 750 nm for $N_{\text{PS266}}/N_{\text{PS500}} = 5:1$.

Comparing Figure 6 with Figure 7, we can see that the influence of differently sized particles on the turbidity measurement for mix 1 is more serious than that for mix 2. This should be associated with the fact that the particle sizes of mix 1 are smaller than those of mix 2. We can also see that the increase in the portion of smaller particles for improving the measuring accuracy looks more effective for mix 1 than for mix 2.

As mentioned above, if the wavelength of the blind point can be determined, we need to know only B and C in eq 6 to achieve K_{D12} . However, it is difficult to experimentally determine the wavelength of the blind point to high accuracy because of the low signal-to-noise ratio near the blind point.

The measured home-coagulation rate constants of PS115, PS266, and PS500 and heterocoagulation rate constants of mix 1 and mix 2 are all given in Table 2. The relevant values of the home-coagulation rate constant estimated by Smoluchowski theory, in which hydrodynamic interactions and inter-particle forces are totally disregarded, is $12.3 \times 10^{-18} \text{ m}^3/\text{s}$ (at 25 °C).

6. Effect of Multiple Scattering on the Turbidity Measurement. When large particles are used in the turbidity measurement, the light transmission becomes rather low, as for the case of PS spheres with a radius of 500 nm used in this study. If low light

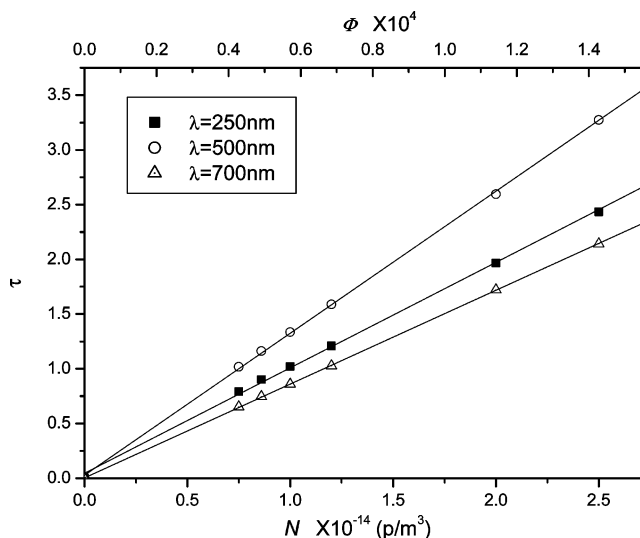


Figure 8. Plots of the turbidity τ vs number concentration N and volume fraction Φ for the largest particles (PS500, radius = $0.5 \mu\text{m}$) and the highest volume fraction (1.0×10^{-4}) used in this study at different wavelengths. The bottom abscissa axis designates the particle number concentration, and the top axis designates the volume fraction.

transmission is primarily associated with multiple scattering, the experimental results would be greatly distorted. In this regard, we have carefully evaluated the possibility of the effect of multiple scattering on the measurement in this work and confirm that this effect should be negligible for the following reasons:

(a) The quasi-crystalline approximation has been used by Vladimir to estimate the effect of multiple scattering on turbidity.²⁵ The result shows that the turbidities calculated with the single scattering approximation and with multiple scattering have a relative difference smaller than 0.7% at the volume concentration of 0.1% for particles like those used in our study. The volume concentrations used in our study (Table 1) is much smaller than 0.1%.

(b) In experimental practice, we also have a criterion to define whether the effect of multiple scattering on the turbidity measurements is important. The turbidity of a stabilized suspension without the effect of multiple scattering can be expressed by $\tau = NC$, where N is the particle number concentration and C is the extinction cross section of a single particle. By varying N , apparently, if τ is linearly related to N , the effect of multiple scattering should be negligible. Figure 8 plots turbidity τ versus number concentration N and volume fraction Φ for the largest particles (PS500, radius = $0.5 \mu\text{m}$) with the highest volume fraction (1.0×10^{-4}) used in this study at different wavelengths. Actually, all data presented in this article were experimentally obtained in the linear region of τ versus N . Therefore, low light transmissions are primarily due to the much higher scattering intensity for large particles, which is not associated with the multiple scattering.

V. Simple Scheme to Obtain the Turbidity Change Rate versus Wavelength

Experimentally determining turbidity derivatives with respect to time ($d\tau/dt$) (that is proportional to the relative coagulation rate) over a range of operating wavelengths is very helpful for more accurately and effectively evaluating the coagulation rate by turbidity measurement. When we have a rough-and-ready curve of ($d\tau/dt$) versus λ beforehand, we can easily select an appropriate wavelength to use in performing the turbidity

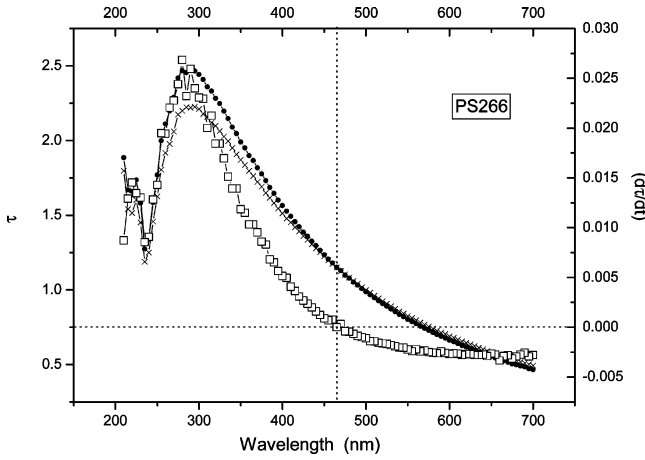


Figure 9. Curves of τ vs λ and the associated curve for $(d\tau/dt)$ vs λ for PS266.

measurement not only apart from the blind point but also with enough sensitivity to the coagulation. Here we present a simple scheme to produce such a curve by means of the spectrophotometer.

Now we use $\tau(t = 0)$ and $\tau(t = \Delta t)$ to denote the values of the turbidity of the dispersion at times $t = 0$ and $t = \Delta t$ at a wavelength of $\lambda = \lambda_1$, respectively, in the turbidity measurement. The turbidity derivatives with respect to time $(d\tau/dt)$ can be evaluated by finite differences:

$$\frac{d\tau}{dt} \approx \frac{[\tau(t = \Delta t) - \tau(t = 0)]}{\Delta t} \text{ at } \lambda = \lambda_1 \quad (8)$$

Suppose at time $t = 0$ that the spectrophotometer starts the turbidity scan over n wavelength points from λ_1 to λ_n and after the time period Δt the first scan finishes and then the second scan immediately follows. After the first scan ends, the turbidity at the i th wavelength point λ_i can be expressed by the following equation:

$$T_i = \tau\left(t = \frac{(i-1)\Delta t}{n}\right) \text{ at } \lambda_i \quad (i = 1, 2, \dots, n) \quad (9)$$

After the second scan finishes, the turbidity derivatives with respect to time at the wavelength λ_i can be achieved by the following approximation

$$\left(\frac{d\tau}{dt}\right)_i \approx \frac{\left[\tau\left(t = \frac{(i-1)\Delta t}{n} + \Delta t\right) - \tau\left(t = \frac{(i-1)\Delta t}{n}\right)\right]}{\Delta t} \quad (i = 1, 2, \dots, n) \quad (10)$$

We are concerned here with only the initial stage of the coagulation process. As long as at this stage the turbidity is linearly related to time, then eq 10 should hold well. Actually, we can perform the third, fourth, and higher scans to get a time series of values of derivatives for each wavelength point.

One of the advantages of this scheme is that all derivatives derived from this approach over different wavelengths are based on the same sample and the same experiment condition. Therefore, the errors due to changes in the sample or experimental conditions are excluded to a great extent. Figure 9 gives the plot of τ versus λ and the associated curve for $(d\tau/dt)$ versus λ , respectively, for PS266. Figure 10 presents similar plots for the mix 1 case.

A problem with this scheme is that all turbidities at different wavelength points are measured at different time points. In other words, supposing $\Delta t = 4$ s, if the first value of τ at λ_1 is measured

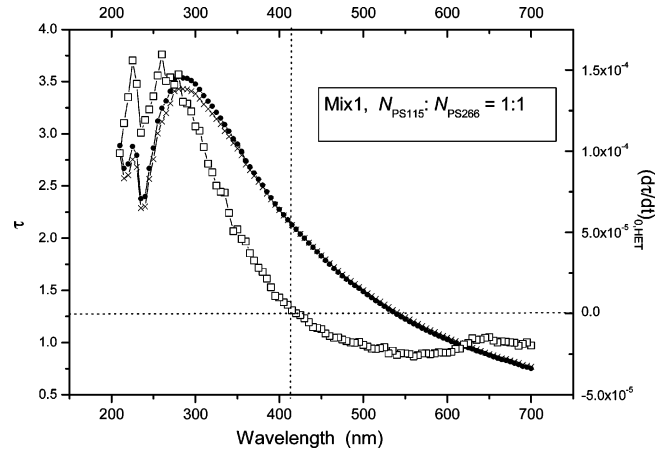


Figure 10. Curves of τ vs λ and the associated curve for $(d\tau/dt)$ vs λ for mix 1 with PS115/PS266 = 1:1.

at zero seconds (the very beginning of the coagulation process), then the first value of τ at λ_n will be measured at the end of four seconds. Apparently, this time delay will deteriorate the accuracy of the obtained values of $(d\tau/dt)$ unless there is a perfectly linear relationship between the turbidity and time. To improve this situation, we can either lengthen the coagulation time by reducing the concentration of the dispersion or shorten Δt by such by narrowing the wavelength range or lessening the wavelength points to be scanned.

VI. Conclusions

Through a theoretical analysis and experimental tests, this article explores a number of important aspects for dealing with the turbidity measurement in determining the absolute heterocoagulation rate constant. The main points can be summarized as below.

The turbidity measurement of the coagulation rate relies on the change in turbidity with the coagulation process. Therefore, it should be performed at a wavelength away from the blind point (zero sensitivity) with sufficient sensitivity to detect the coagulation rate. However, for heterocoagulation the blind point shifts with the component fraction, although for homocoagulation it is definite.

Because turbidity increases radically with particle size, larger particles may significantly dominate the turbidity behavior of the binary dispersion, resulting in a large measurement error. This tendency becomes stronger when constituent particles of the dispersion are smaller. Increasing the component fraction of small particles properly is favorable for improving this situation.

Similarly with homocoagulation, to achieve a more accurate rate constant of heterocoagulation by turbidity measurement, using larger particle is more preferable. The T-matrix method can be used to correctly evaluate the relevant extinction cross sections of doublets formed during heterocoagulation without the limitation on particle size, but all previous theories are applicable only to small particles.

Finally, we described a simple scheme to obtain a rough-and-ready curve of the rate of turbidity change versus wavelength that is helpful in selecting an appropriate wavelength for performing the turbidity measurement.

Acknowledgment. This work is supported by grants 10672173, 10332050, and 20473108 from the National Natural Science Foundation of China and the ‘‘Chuang-xin Project’’ of the Chinese Academy of Sciences.